L. E. Gurrieri, C. Squires, S. Noghanian, and T. Willink, “High resolution spatiotemporal characterization of electric field polarization for indoor wireless environments,” in Canadian Conference on Electrical and Computer Engineering, 2006. CCECE'06, pp. 1462–1465, 2006. DOI: 10.1109/CCECE.2006.277655, ISBN: 1-4244-0038-4

HIGH RESOLUTION SPATIOTEMPORAL CHARACTERIZATION OF ELECTRIC FIELD POLARIZATION FOR INDOOR WIRELESS ENVIRONMENTS

L. E. Gurrieri[1], C. Squires[2], S.Noghanian[1], T. Willink[2],
[1] *University of Manitoba,* [2] *Communications Research Centre*
e-mail: lgurrier@ee.umanitoba.ca

Abstract

The effects of the electric field polarization on the received power are investigated based on high resolution measurements of the indoor wireless channel. The results presented here were obtained using a channel sounding testbed, which was specially designed to study the radio propagation in the 5-6 GHz frequency band with high resolution in terms of angle-of-arrival (AOA) and time-of-arrival (TOA). Measurements were made at different indoor locations and the influence of the receiver surroundings on polarization cross-coupling was analyzed as a function of the azimuthal and elevation AOA. Significant cross-coupling was measured in locations where multipaths arrive with oblique AOA with respect to the horizontal plane ($\theta = 90^o$). The cross-polarization was characterized with high resolution in azimuth and elevation, which enabled the study of the spatial distribution of depolarized multipaths. The amount of power due to cross-polarized multipaths was estimated for a vertically polarized transmitter antenna located in different indoor environments. The advantages of using multi-element antennas and polarization diversity were made evident, as well as the importance of the relative location of transmitter and receiver and the 3-D distribution of the nearest scatterers.

Keywords *— MIMO systems, wireless indoor channels characterization, propagation, electromagnetics, polarization.*

1 Introduction

The polarization characterization of indoor channels is relevant not only in the design of polarization diversity systems but also as a means to quantify the losses incurred by considering only the co-polarized signals in existing links. We carried out a measurement campaign aiming to fill a gap in the experimental information available regarding the cross-polarization of electromagnetic waves in the 5-6 GHz band. Early studies performed at lower frequencies are not well suited to describing the behaviour of indoor channels at frequency bands and data rates of interest nowadays [4]. Early ray-tracing simulations at lower frequencies reported that, when vertically polarized antennas are used at both sides of the link, cross-polarization losses may be ignored [8]. This conclusion is true only for AOAs restricted to the horizontal plane. In our measurements, we found a significant amount of cross-coupling above and below the horizontal plane in non-line-of-sight (NLOS) environments. In this paper we will introduce our results in terms of the amount of cross-polarization as a function of the AOA.

Multi-input multi-output (MIMO) is just one example of the next generation of communication systems that may take advantage of the polarization diversity created in indoor environments to boost the achievable capacity [8]. Technology trends demand innovative solutions to achieve wireless data rates that were unthinkable a few years ago. This work may bring new insights into the subject of indoor cross-polarization that ultimately may help in the design and improvement of high data rate communication systems for indoor links.

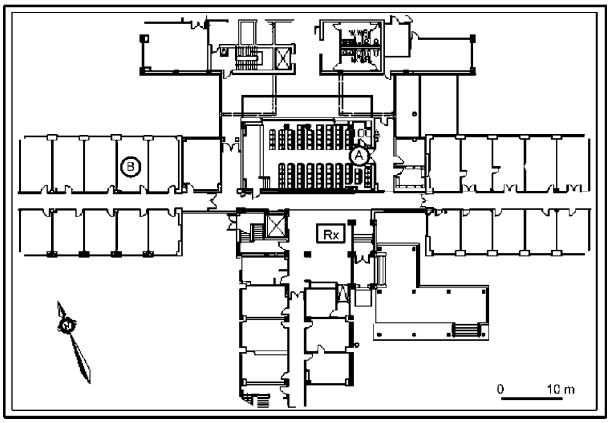

Figure 1. Transmitter locations A and B, and receiver location Rx

2 Channel Sounding Technique

The channel complex impulse response (CIR) was measured using a network analyzer and a specially designed receiver antenna system that allows us to scan the radio environment for selective AOAs. The acquisition apparatus consists of a square planar array of 8 by 8 elements with a pencil-like radiation pattern, 10^o half-power beamwidth (HPBW), -20 dB sidelobe levels, and 1 GHz bandwidth (BW) (4.9-5.9 GHz). The experiments were performed in the 5.10-5.85 GHz frequency range. This band was chosen because of its relevance to current wireless LANs.

The channel sounding technique has a 2 ns time resolution which allows us to resolve multipaths with a path difference of 40 cm. Special consideration was made to diminish the near-field effects caused by the indoor clutter in the receiver surroundings. A biconical antenna located at the chosen test points (Fig. 1) was used to transmit a continuous wave (CW) which was swept across the BW of

interest in 1.875 MHz frequency steps.

On the receiver side, a PC controlled system positioned the wideband antenna to the desired azimuth (ϕ) and elevation (θ) angles. In the system of coordinates used, $\theta = 0^o$ corresponds to the vertical axis perpendicular to the floor plane pointing on the ceiling direction. The scanning was performed from 0^o to 355^o in ϕ and from 30^o to 150^o in θ, both in steps of 5^o. Five channel snapshots were acquired at each look angle, and then stored automatically. The whole process was monitored remotely to reduce the chances of perturbing the channel measurement. The snapshots of the channel were acquired at half of the HPBW, obtaining four correlated sets of realizations of the CIR. We further use these data to extrapolate a high resolution spatial-temporal estimation of each CIR using deconvolution techniques (CLEAN) [5] and 2-D signal processing [6].

3 Locations

The two NLOS locations chosen for this experiment are shown in Fig. 1. The selection of location A was made based on the distribution of potential scatterers around the receiver area and location B was chosen to include an example of a typical office space scenario. Location A is an auditorium with folded metallic chairs and plenty of potential scatterers. On the other hand, location B is a fully furnished office space which represents a completely different environment for radio propagation. Heating ducts, pipes and electric wires run above the ceiling. Double layer plywood, concrete and brick walls, steel reinforced concrete columns as well as typical office equipment are present in both test locations. The distinctive characteristic of a real indoor scenario in comparison with a simulated environment commonly used in ray-tracing simulations lies in the effects of tens of potential scatterers such as indoor clutter, structural details, etc. In order to have maximum control over the variables that could affect the channel measurement, we conducted the tests during the weekend when the personnel in the test area was minimum.

4 Processing of Data

Each of the individual channel multipath components (MPC) were extracted from the acquired CIR using the false alarm rate criteria originally proposed in [7]. The large BW used in the experiment reduced the number of irresolvable MPCs that may be combined in each time bin causing channel fading.

The CIR for each AOA acquired by our scanning system can be modeled as

$$h_i(\theta,\phi,\tau) = \sum_{n=1}^{N_\theta}\sum_{m=1}^{N_\phi}\sum_{k=1}^{N_\tau}\beta_i(n,m,t)\delta(\theta-\theta_n)\delta(\phi-\phi_m)\delta(\tau-\tau_k) \quad (1)$$

where δ is the Dirac's delta function, the index i, such that $i = V, H$, is used to denote vertical or horizontal polarization, respectively, $\beta_i(n,m,k)$ is the complex amplitude of the k^{th} multipath, N_ϕ, N_θ, and N_τ are the total number of resolution bins in azimuth, elevation and delay, respectively, θ_n and ϕ_m specify the look angle, and τ_k is the delay of the k^{th} multipath.

Using the CIR defined in (1), the total received coherent power as a function of the AOA can be estimated as

$$P_i^c(\theta,\phi) = \int_{\tau=0}^{T} |h_i(\theta,\phi,\tau)|^2 d\tau \quad , \; i: V, H \quad (2)$$

where T is the channel capture interval. The total coherent power as a function of the azimuth and elevation is defined as follows

$$P_i^c(\theta) = \int_{\tau=0}^{T}\int_{\phi=0^o}^{360^o} |h_i(\theta,\phi,\tau)|^2 d\phi d\tau \quad , \; i: V, H \quad (3)$$

$$P_i^c(\phi) = \int_{\tau=0}^{T}\int_{\theta=30^o}^{150^o} |h_i(\theta,\phi,\tau)|^2 d\theta d\tau \quad , \; i: V, H. \quad (4)$$

The total noncoherent power as a function of the elevation and azimuth is defined as

$$P_i^{nc}(\theta) = \int_{\tau=0}^{T} \left| \int_{\phi=0^o}^{360^o} h_i(\theta,\phi,\tau) d\phi \right|^2 d\tau \quad , \; i: V, H \quad (5)$$

$$P_i^{nc}(\phi) = \int_{\tau=0}^{T} \left| \int_{\theta=30^o}^{150^o} h_i(\theta,\phi,\tau) d\theta \right|^2 d\tau \quad , \; i: V, H. \quad (6)$$

The distinction between the total coherent and noncoherent power is made here to compare the performance achievable by multi antenna systems (MIMO) versus single antennas in polarization-based communication systems.

We used the cross-polarization coupling (XPOL) to quantify the amount of received power that is received in a polarization state orthogonal to its original transmitted mode [1]. This coupling effect may happen due to interactions with the environment, i.e., walls, floors and indoor clutter after reflections, transmissions and diffractions of the transmitted signal. When vertically polarized antennas are used at both sides of the link, which is common practice in indoor communications, the XPOL may be used as a measure of the amount of power that arrives at the receiver location as horizontally polarized MPCs. The XPOL as a function of the AOA can be defined as

$$XPOL(\theta,\phi) = \frac{P_H^c(\theta,\phi)}{P_V^c(\theta,\phi)} \quad (7)$$

where P_H and P_V were defined in (2). In order to study the depolarization in azimuth and elevation using coherent and noncoherent power addition, we defined

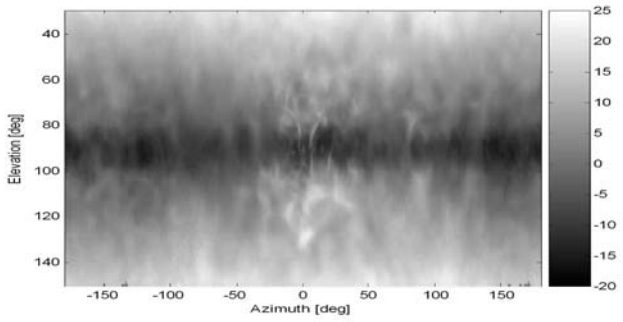

(a) Location A

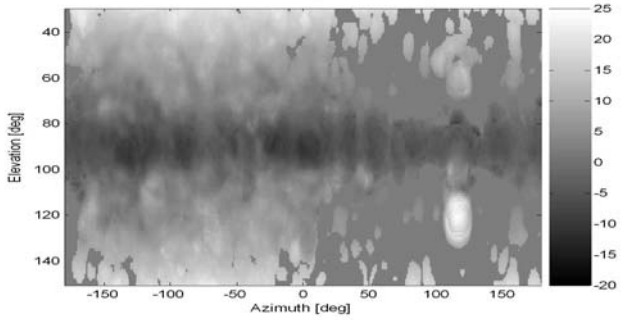

(b) Location B

Figure 2: XPOL(θ, ϕ).

$$XPOL(\theta) = \frac{P_H(\theta)}{P_V(\theta)} \tag{8}$$

$$XPOL(\phi) = \frac{P_H(\phi)}{P_V(\phi)} \tag{9}$$

where P_V and P_H were defined in (3)-(4) for coherent power and in (5)-(6) for noncoherent power.

5 Results

Location A is an example of a dense channel where the arrival times between MPCs are smaller than the resolvable bin width. The large number of scatterers in this environment creates reflections from ceiling and floors, increasing polarization decoupling for high and low elevation AOAs. The maximum XPOL coupling was created by the contribution of oblique reflected MPCs coming from the floor at low angle as shown in Fig. 2(a).

Location B, in contrast, is an example of a sparse channel where the MPC interarrival times are larger than the bin width. The topology of location B is comparable to a dielectric canyon which acts as a lossy waveguide favouring the propagation of vertically polarized components. Horizontally polarized multipaths caused by interactions in the transmitter surroundings arrive highly attenuated at the receiver. Therefore, the XPOL measured can be attributed to the decoupling of vertical components arriving in the receiver area from $\theta = 90^o$ (horizontal plane) after one or more interactions with the walls. The maximum depolarization was symmetrically located in two clusters above and below the horizontal plane around $\phi = 120^o$ as shown in Fig. 2(b). Oblique reflections on two metal panels perpendicularly oriented with respect to the wall explain the maximum XPOL concentration observed for that AOA. The AOAs of cross-polarized MPCs show a distinctive pattern in both locations which is evident in Fig. 2. Note that the maximum XPOL not necessarily implies stronger horizontally polarized MPCs. The presence of weaker or the complete absence of vertically polarized MPCs explains the higher XPOL regions. Furthermore, analyzing the power distribution of horizontally polarized multipaths, we found strong clusters of cross-polarized MPCs located closer or even into the region of minimum decoupling ($\theta = 90^o$).

Fig. 3 shows the amount of decoupling as a function of azimuth and elevation AOA individually for both locations

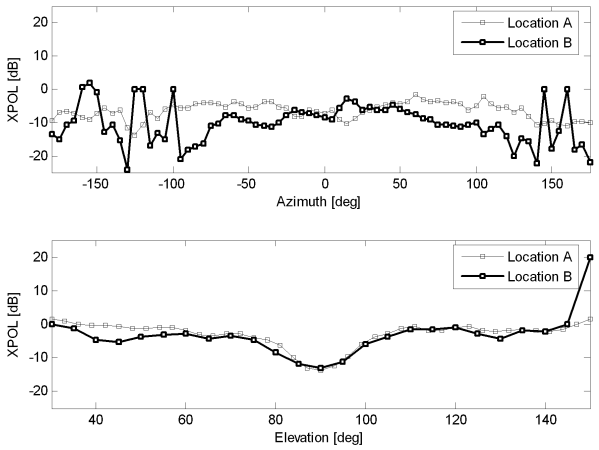

Figure 3: XPOL: coherent multipath combination

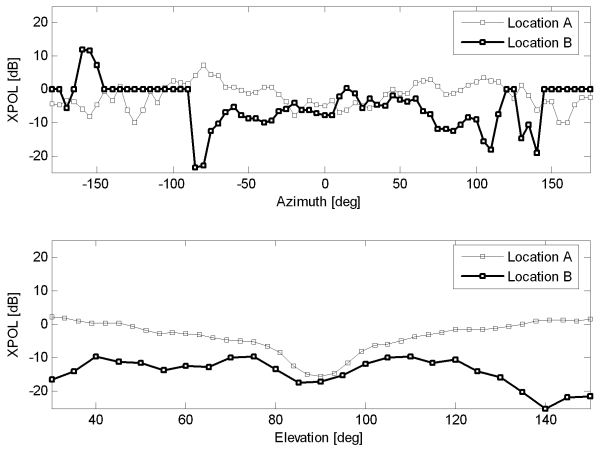

Figure 4: XPOL: noncoherent multipath combination

TABLE I
Comparative results (Non-Coherent Addition)

	Rx Power	Ver. Pol	Hor. Pol	XPOL
A	-16.1 dBm	81.2 %	18.7 %	-7.2 dB
B	-19.2 dBm	87.2 %	12.7 %	-8.9 dB

TABLE II
Comparative results (Coherent addition)

	Rx Power	Ver. Pol	Hor. Pol	XPOL
A	-10.1 dBm	73.8 %	26.1 %	-5.8 dB
B	-15.2 dBm	91.1 %	8.8 %	-10.5 dB

estimated using the cumulative received power defined in (8)-(9). In both cases, the maximum decoupling occurs for MPCs coming from the ceiling and floors ($\theta < 40^o$ and $\theta > 100^o$) and the minimum depolarization is observed in region $\pm 10^o$ of the horizontal plane. Notice that similar decoupling is observed for signals coming from location A for coherent and noncoherent multipath combination (Fig. 3-4). In contrast, decoupling is highly reduced in those MPCs coming from location B with sharp elevation angle for the noncoherent case (Fig. 4) which shows the limitation in the potential use of those decoupled MPCs by a narrow band system.

Tables I and II show the quantitative results for the total XPOL estimated for each location. The percentage of the total power received from horizontally polarized MPCs is larger in location A than in location B for coherent and non-coherent MPC addition. For location A, the coherent addition of multipaths enhances the XPOL about 8 %, while the opposite effect is observed for location B with 6 % XPOL decrease.

6 Conclusions

In these experiments, we found a strong dependency of the cross-polarization of multipath components on the elevation AOA. While vertically polarized multipaths are confined exclusively to the region around the horizontal plane, cross polarized MPCs can have sharp AOAs. In rich scattering environments, MPCs are expected to arrive at the receiver location after one or more interactions with the surroundings. When the number of these interactions is low, it is more likely that the strongest MPCs make their way to the receiver area. Furthermore, if these MPCs have elevation AOAs outside the horizontal plane, the probability of oblique reflections on the floor and ceiling close to the receiver is higher and so is the creation of cross-polarized MPCs. A vertically polarized wave will arrive at the receiver location co-polarized and confined mostly to the horizontal plane due to the wave guide effect of walls: this is the case in location B. Therefore, the probability of having cross-polarized components from scattering in the receiver surroundings is less than that of MPCs arriving after being subject to first or second order scattering and coming from above and below the horizontal plane, as in location A. It can be concluded that scatterers located in the neighbourhood of the receiver and the relative transmitter-receiver location play an important role in terms of the creation of depolarized MPCs.

A strategy to boost the capacity of a MIMO system might be to increase the total received signal-to-noise ratio (SNR) by collecting the otherwise wasted power due to cross-polarized MPCs. It is left for the future work to quantify the performance improvement achievable for a system such as the one proposed.

Acknowledgments

The work reported herein was supported by Defence Research and Development of Canada (DRDC) and National Research Council Canada (NSERC). The authors thank the Advanced Antenna Technology research group for their assistance.

References

[1] D. Chizhik, J. Ling, R.A. Valenzuela, "The effects of electric field polarization on indoor propagation," *IEEE 1998 International Conference on Universal Personal Communications*, ICUPC '98, vol. 1, 5-9 pp. 459-462, Oct. 1998.

[2] D. D. Cox, R. R. Murray, H. W. Arnold, A. W. Norris, and M. F. Wazowicz, "Cross-Polarization coupling measured for 800 MHz radio transmission in and around houses and large buildings," *IEEE Trans. on Antenna and Propagation*, vol. AP-34, no. 1, pp. 83-87, Oct. 1998.

[3] K. Kalliola, K.Sulonen, H. Laitinen, O. Kivekas, J.Krogerus, P. Vainikainen, "Angular power distribution and mean effective gain of mobile antenna in different propagation environments," *IEEE Trans. Veh. Technol.*, vol. 51, no. 5, pp. 823-838, Sep. 2002.

[4] A.F. Molisch, "Ultrawideband propagation channels-theory, measurement, and modeling," *IEEE Trans. Veh. Technol.*, vol. 54, no. 5, pp. 1528-1544, Sep. 2005.

[5] R. Bose, A. Freedman, B. Steinberg, "Sequence CLEAN: A modified deconvolution technique for microwave images of contiguous targets," *IEEE Trans. on Aerospace and Electronics Systems*, vol. 38, no. 1, pp. 89-96, Jan. 2002.

[6] R. C. Gonzalez, P. Wintz, *Digital image processing, 2nd ed.* Addison-Wesley, Nov. 1987.

[7] E. Sousa, V. M. Jovanović, C. Daignaeult, "Delay spread measurents for the digital cellular channel in Toronto," *IEEE Trans. Veh. Technol.*, vol. 43, no. 4, pp. 837-847, Nov. 1994.

[8] P. Kyritsi, D. Cox, R. A. Valenzuela, P. W. Wolniansky, "Effect of antenna polarization on the capacity of a multiple element system in an indoor environment," *IEEE J. Selected Areas in Commun.*, vol. 20, no. 6, pp. 1227-1239, Aug. 2002.